

Probabilistic Flow Connectivity Mapping with 4D flow MRI data for the Assessment of Blood Mixing in Fontan Circulation

Kelly Jarvis^{1,2}, Susanne Schnell¹, Pim van Ooij¹, Alex Barker¹, James Carr¹, Joshua D Robinson^{3,4}, Cynthia Rigby^{1,5}, and Michael Markl^{1,2}

¹Radiology, Northwestern University, Chicago, IL, United States, ²Biomedical Engineering, Northwestern University, Chicago, IL, United States, ³Pediatrics, Northwestern University, Chicago, IL, United States, ⁴Cardiology, Ann & Robert H Lurie Children's Hospital of Chicago, Chicago, IL, United States, ⁵Medical Imaging, Ann & Robert H Lurie Children's Hospital of Chicago, Chicago, IL, United States

Introduction: Patients with only one fully functioning ventricle undergo multiple surgical interventions to create a Fontan circulation, where upper and lower venous return is routed directly to the lungs through the pulmonary arteries. Non-uniform blood distribution from the superior and inferior vena cava, SVC and IVC, to the left and right pulmonary arteries, LPA and RPA is suspected to cause arteriovenous malformations, leading to negative outcomes¹. Blood mixing (distribution of caval venous flow to the left and right lungs) can be quantified from the velocity vector fields acquired by 4D flow MRI. However, the acquired blood flow velocities include measurement noise uncertainties that can affect the magnitude and orientation of the measured velocity vector field. Most previous studies using in-vivo 4D flow MRI data have used 3D blood flow visualization based on single streamlines or pathlines and did not account for the underlying velocity noise. Recently, a new approach utilizing 3D probabilistic flow connectivity mapping has been presented that directly integrates local estimates of velocity noise into the analysis to report the level of statistical accuracy in 3D visualization². It was the aim of this study to systematically analyze 3D probabilistic flow connectivity mapping and the influence of velocity noise on pathline visualization for a synthetic Fontan phantom. In addition, this method was utilized for the evaluation of a patient with Fontan circulation to assess blood mixing while incorporating measurement uncertainty.

Theory: To fully account for the inherent noise-related uncertainties in 4D flow MRI data, 3D probabilistic flow connectivity mapping is based on the distribution of possible flow trajectories. The trajectory of a conventional pathline in a vector field can be described by a train of spatio-temporal vectors (s_k) starting at a spatio-temporal emitter point (x_0) (Figure 1: left). When noise is taken into account, vectors (s_k) and positions (x_k) become random variables. A large number of possible flow pathways ("probabilistic pathlines") can thus originate from a single emitter point (Figure 1: right). A series of probabilistic pathlines generated by repeat calculation of flow trajectories with varying local measurement uncertainty can be used to derive the velocity noise induced uncertainty for flow pathways in the global image.

Methods, simulations: 3D probabilistic flow connectivity mapping was developed for a synthetic Fontan phantom velocity dataset (V_x, V_y, t) with preferential flow to the RPA (Figure 2a-c) (Matlab, The MathWorks, USA). Time-resolved pathlines were calculated from a total of $N_{em} = 20$ emitter points evenly distributed across the IVC to establish flow pathways at noise level 0, which was considered the ground truth. Random Gaussian noise distributions were generated with standard deviations = 5% and 10% of a typical velocity sensitivity of 1 m/s for noise levels 1 and 2. Noise was added independently to each voxel and velocity component (V_x, V_y). Pathlines were calculated for all 20 emitter points in the IVC. Pathline calculation was repeated $N_{exp} = 100$ times with newly generated noise distributions to derive probabilistic pathlines as shown in Figure 3. For each pathline calculation, mixing ($M_{RPA,LPA}(i)$ for $i=1$ to N_{exp}) was calculated by counting the number of probabilistic pathlines reaching the RPA or LPA and normalizing to the total number reaching either side. Probabilistic mixing was quantified as the average of the individual mixing results (eq 1) and mixing uncertainty was determined by the standard deviation of mixing between probabilistic pathlines (eq 2).

Methods, in-vivo analysis: 4D flow MRI (spatial resolution = $2.3 \times 1.8 \times 2.8$ mm³, temporal resolution = 40.8 ms, $v_{enc} = 1$ m/s) with whole heart coverage was performed in a 1.5T system (Avanto, Siemens, Germany) in 1 patient (male, age 5) with extra-cardiac Fontan circulation. A time-averaged 3D phase contrast angiogram (PC-MRA) was calculated using 4D flow MRI data to provide an enhanced depiction of cardiovascular geometry. 3D segmentation (Mimics Innovation Suite, Materialise, Belgium) was performed to create a 3D geometry of the Fontan connection (Figure 4a). Standard mixing results were obtained using the single conventional pathline calculation method (Ensign, CEL, Apex, NY) (Fig 4b). Distributions at noise level 1 and 2 were added to the dataset and probabilistic pathlines were calculated (Figure 4c,d). In addition, the true noise in the measured velocity data was estimated by the standard deviation of the velocities in an area of no flow.

Results: Figure 3 and table 1 summarize the results of the simulation of probabilistic mixing in a model Fontan connection. Compared to the true mixing (60% flow to the RPA, 40% to the LPA), probabilistic analysis results in similar mean probabilistic mixing for both noise levels but noticeable mixing uncertainty which, as expected, was increased for noise level 2 [Table 1]. For the in-vivo data (Figure 4), mean probabilistic mixing indicated preferential flow from the IVC to the RPA and thus non-uniform distribution of protein rich hepatic blood to the left and right lungs. The small mixing uncertainties indicate the stability of the probabilistic mixing analysis (Figure 4d). The true noise level ($sd = 0.018$ m/s) was 36% and 18% of noise levels 1 and 2 used for mixing analysis.

Conclusions: The 3D probabilistic flow connectivity mapping methods developed here demonstrated the effects of measurement noise on mixing results for the quantification of blood distribution in Fontan circulation. For the synthetic data, mean probabilistic mixing could be successfully used for a robust estimation of the true underlying mixing (60%, 40%) for both noise levels. However, the large mixing uncertainty, up to 20-30% of the flow reaching the LPA and RPA, indicate that a single pathline calculation alone can lead to substantial errors in mixing quantification. Probabilistic pathlines thus offer a robust new tool for flow pathway calculation in the presence of noise and are thus less sensitive to potential errors due to velocity noise uncertainties. After adding noise to the synthetic dataset, some pathlines did not reach either side because they were terminated when they reached an area of zero velocity, highlighting the potential effect of noise on velocity data visualization. For in-vivo data, conventional and probabilistic pathline calculations detected a similar division of blood flow into the LPA and RPA in a patient with Fontan circulation. However, the 3D probabilistic flow connectivity mapping method also provided an insight into the uncertainty of the mixing measurement.

References: 1. Shah MJ, et al. *Ann Thorac Surg.* 1997;63:960-3.

2. Friman O, et al. *Med Image Anal* 2011;15:720-728.

Grant support by NIH NHLBI grant R01HL115828

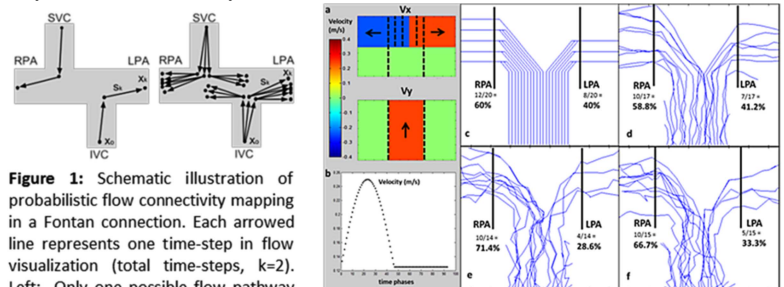


Figure 1: Schematic illustration of probabilistic flow connectivity mapping in a Fontan connection. Each arrowed line represents one time-step in flow visualization (total time-steps, $k=2$). Left: Only one possible flow pathway ignoring velocity noise. Right: Probabilistic pathlines for $N_{exp} = 3$ pathline calculations with varying local measurement uncertainty.

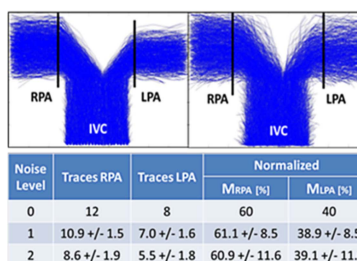


Figure 3: Pathline results from noise level 1 (left) and level 2 (right). **Table 1 –** Mixing results for the synthetic dataset. $N_{em} = 20$, $N_{exp} = 100$.

Equations:

$$1. \quad M_{RPA} = \frac{1}{N_{exp}} \sum_{i=1}^{N_{exp}} M_{RPA}(i), \quad M_{LPA} = \frac{1}{N_{exp}} \sum_{i=1}^{N_{exp}} M_{LPA}(i)$$

$$2. \quad \sigma_{M_{RPA}} = \sqrt{\frac{\sum_{i=1}^{N_{exp}} (M_{RPA}(i) - M_{RPA})^2}{N_{exp}}}, \quad \sigma_{M_{LPA}} = \sqrt{\frac{\sum_{i=1}^{N_{exp}} (M_{LPA}(i) - M_{LPA})^2}{N_{exp}}}$$

Figure 2: Pathlines were calculated for the (a) synthetic velocity dataset with (b) pulsatile velocity by applying (c) noise level 0 (d) noise level 1 (e) noise level 2 and (f) noise level 2 repeated. The percent of probabilistic pathlines reaching the RPA or LPA varied with different noise levels (d vs. e) and when repeating the experiment with the same level of noise (e vs. f).

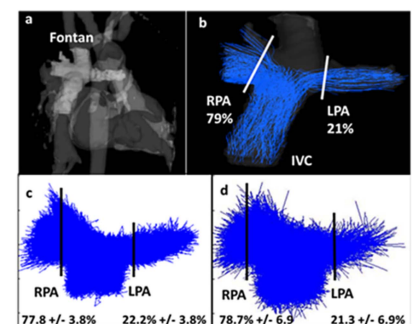


Figure 4: After the segmentation of the (a) 3D PC-MRA, the (b) standard mixing analysis was performed in the Fontan geometry. Probabilistic pathlines were calculated for (a) noise level 1 and (b) noise level 2. $N_{em} = 148$, $N_{exp} = 100$.